Changes in luminescence intensities and carrier dynamics induced by proton irradiation in $In_xGa_{1-x}As/GaAs$ quantum dots

S. Marcinkevičius and J. Siegert
Department of Microelectronics and Information Technology, Royal Institute of Technology, Electrum 229, 164 40 Kista, Sweden

R. Leon
Jet Propulsion Laboratory, California Institute of Technology, 4800 Oak Grove Drive, Pasadena, California 91109

B. Čechavičius
Semiconductor Physics Institute, Goštauto 11, 2600 Vilnius, Lithuania

B. Magness and W. Taylor
Department of Physics and Astronomy, California State University, Los Angeles, California 90032

C. Lobo
Cavendish Laboratory, University of Cambridge, Cambridge CB3 0HE, United Kingdom
(Received 25 July 2002; revised manuscript received 14 October 2002; published 17 December 2002)

The effects of proton irradiation (1.5 MeV) on photoluminescence intensities and carrier dynamics were compared between InGaAs/GaAs quantum dots and similar quantum well structures. A significant enhancement in radiation tolerance is seen with three-dimensional quantum confinement. Measurements were carried out in different quantum dot structures varying in dot surface density ($4\times10^8-3\times10^{10}$ cm^{-2}) and substrate orientation [(100) and (311)*B*]. Similar trends were observed for all quantum dot samples. A slight increase in photoluminescence emission intensity after low to intermediate proton doses is observed in InGaAs/GaAs (100) quantum dot structures. The latter is explained in terms of more efficient carrier transfer from the wetting layer via radiation-induced defects.

DOI: 10.1103/PhysRevB.66.235314 PACS number(s): 78.66.Fd, 78.55.−m, 78.47.+p

I. INTRODUCTION

Semiconductor quantum dots (QD's) have been the focus of extensive research due to their appealing electronic and optical properties, which have allowed successful implementations of several emerging device applications. QD based devices include novel QD lasers, broadband QD infrared photodetectors, different types of semiconductor QD memories,[1,2] and highly parallel computing architectures[3] based on quantum dot cellular automata. Recent developments have shown rapid progress in the implementation of some of the advantages of QD based lasers predicted by theory[4] demonstrating reductions in threshold-current densities[5,6] and an order of magnitude lower chirp.[7] Likewise, QD based infrared photodetectors have shown broader band absorption, and the ability of incident light absorption expected from the different selection rules between QD's and quantum wells (QW's).[8]

Protons can cause displacement damage and structural defects in semiconductor devices, resulting in performance degradation and failure. Minimizing the impact of radiation-induced degradation in optoelectronic devices is therefore important for several applications, and it can include the exploitation of inherent radiation hardness in quantum structures. Some of the fundamental properties of QD's suggest that optoelectronic devices incorporating QD's could tolerate greater radiation damage than other heterostructures. Exciton localization in the quantum dots due to three-dimensional confinement reduces the probability of carrier nonradiative recombination at radiation induced defect centers if damage is created outside the QD region. Recent findings show that indeed, some types of semiconductor quantum dots are very radiation hard, which makes QD based optoelectronic devices ideal for space applications. Recent studies of optical properties in proton, ion, and electron-irradiated quantum dot structures,[9–11] and in ion and proton-irradiated QD lasers[12,13] showed that the QD's structures and QD based devices are much more resistant to radiation induced damage than bulk semiconductors or quantum wells. Some of these studies showed not only better radiation tolerance, but also an increase in either photoluminescence (PL) intensities[9] or laser performance[11] with low proton or ion fluences. A better understanding of the physical processes responsible for this surprising finding was one of the aims of this present work. In order to accomplish such understanding, comparisons of optical emission intensities and carrier dynamics from different types of InGaAs/GaAs dots and wells after irradiation with 1.5-MeV protons were undertaken. Results presented here confirm better radiation tolerance from all the QD's studied, and give insights into the mechanisms for higher PL intensities after radiation exposure observed in some of the QD structures.

II. EXPERIMENTAL DETAILS

InGaAs/GaAs (100) and InGaAs/GaAs (311)*B* QD's were grown by metal-organic chemical-vapor deposition (MOCVD) in a horizontal reactor cell operating at 76 Torr.

 ©2002 The American Physical Society

TABLE I. Data summary for InGaAs/GaAs QD and QW structures used in this study.

Structure and material dot/barrier	Surface density (dots/cm^2)	Average diameter (nm)	Average aspect ratio (height/diameter)	80 K PL peak energy (eV)
Quantum well		1 nm width		1.35
Low density (100) QD's	4×10^8	25 ± 5	1/6	1.06 (ground state)
High density (100) QD's	2×10^{10}	25 ± 5	1/6	1.18
(311)*B* QD's	3×10^{10}	25 ± 5	1/8	1.32

Trimethylgallium, trimethylindium, and arsine were used as precursors. For the QD's, growth of a 50-nm GaAs buffer layer at 650 °C was followed by deposition of 1.5-nm InGaAs with a nominal indium mole fraction of 0.6. Different surface densities of InGaAs QD's in similar sizes were obtained by changing the arsine partial pressures during growth of the QD's.[14] InGaAs quantum well structures were obtained by stopping the growth of InGaAs before the onset of the Stranski-Krastanow transformation, giving a thin (1 nm) QW. InGaAs QD's and QW were capped with GaAs layers, deposited while the temperature was gradually raised to 600 °C. Atomic force microscopy and transmission electron microscopy were used to give information on island sizes and surface densities in capped and uncapped QD's. Proton irradiation was carried out using a Van De Graaff accelerator. Samples were irradiated at room temperature using 1.5-MeV protons at five different doses ranging from 1.3×10^{11} to 3.5×10^{13} cm^{-2}, with a dose rate $\sim6\times10^{12}$ protons/sec. Dose uniformity was monitored using radiochromic film at low doses. Carrier dynamics were studied by time-resolved photoluminescence at 80 K after excitation by a short laser pulse from a self mode-locking Ti: sapphire laser (pulse duration 80 fs, central wavelength 800 nm, repetition frequency 95 MHz). For the PL detection, a synchroscan streak camera with an infrared enhanced photocathode, combined with a 0.25-m spectrometer (temporal resolution 3 ps) was used. The average excitation power was between 1 and 10 μW, corresponding to the laser pulse energy of 0.01–0.1 pJ. The laser spot size was 50 μm in diameter. To assure that the measured PL rise times were not affected by the limited temporal resolution of the streak camera, additional measurements using an upconversion setup with a temporal resolution of 150 fs were carried out. Ternary compositions ($In_{0.6}Ga_{0.4}As$) between QW and QD's were identical, and so were capping layer thicknesses (100 nm for both QD's and QW), therefore these results are not dependent on material or proton energy loss differences.

III. EXPERIMENTAL RESULTS AND SIMULATIONS

Table I presents a summary and description of the different structures used in this study, showing their materials and structural properties (dot sizes, aspect ratios, and concentrations) as well as the wavelength emission at their PL maximum intensity. It can be seen that the emission from the QW is at a higher energy than from the QD's. This is because only very thin dislocation-free QW's (1 nm) can be obtained of the same ternary composition as the QD's. It is worth noting that InGaAs/GaAs (311)*B* QD's have similar diameters, but form in slightly higher surface concentrations with lower aspect ratios than InGaAs/GaAs(100) QD's. Since the dimensions in the growth direction dominate quantum confinement energies, corresponding PL emission peaks are also at higher energies.[15] As shown from the values in this table, the high-density InGaAs QD's exhibit a blueshift of the PL emission energy with respect to the low-density InGaAs QD's. These differences are not seen to correspond to variations in dot sizes or compositions, and have been ascribed to strain deformation of the QD confining potentials, resulting in shallower effective confinement with increasing dot density.[16]

Figure 1 shows the dependence of the peak PL intensity on proton fluences for the QD and the QW samples. The difference between the QW and QD's is striking: At the highest proton fluence, the QW PL intensity is ~30 times lower than for the unirradiated sample, while the QD PL intensity decreases to just a little over half of its original intensity. Moreover, as observed in earlier work,[9] we observe an *increase* in the QD PL intensity for the (100) InGaAs/GaAs QD's (most prominent, up to 50%, in the low-density dots) for small irradiation doses as compared to the unirradiated QD's.

An inset to Fig. 1(b) shows typical PL transients for one of the samples, presented as a function of increasing proton fluence. After a fast rise with a characteristic time of 4–5 ps (not resolved in the figure), the PL decays due to radiative and nonradiative carrier recombination. The PL rise and decay times were extracted from the PL transients using a relation $I(t)\propto[\exp(-t/\tau_r)-\exp(-t/\tau_d)]/(\tau_r-\tau_d)$, where τ_r and τ_d are the PL rise and decay times, respectively. The dependence of the PL decay times on proton fluence is shown in Fig. 2. As shown in the figure, carrier lifetimes in QD's are less affected by proton irradiation than in the QW. For example, the 80-K carrier lifetimes in (311)*B* QD's decrease from 2.2 ns for the unirradiated sample to 1.4 ns for the sample with the highest proton dose, compared to a ~20-fold and ~40-fold decrease for the QW and the wetting layer (WL), respectively.

Figure 3 shows the variations in QD PL rise times for all QD samples, also as a function of increasing proton fluence. It can be seen that QD PL rise times, which reflect carrier capture from the barriers into the dots, decrease with irradiation.

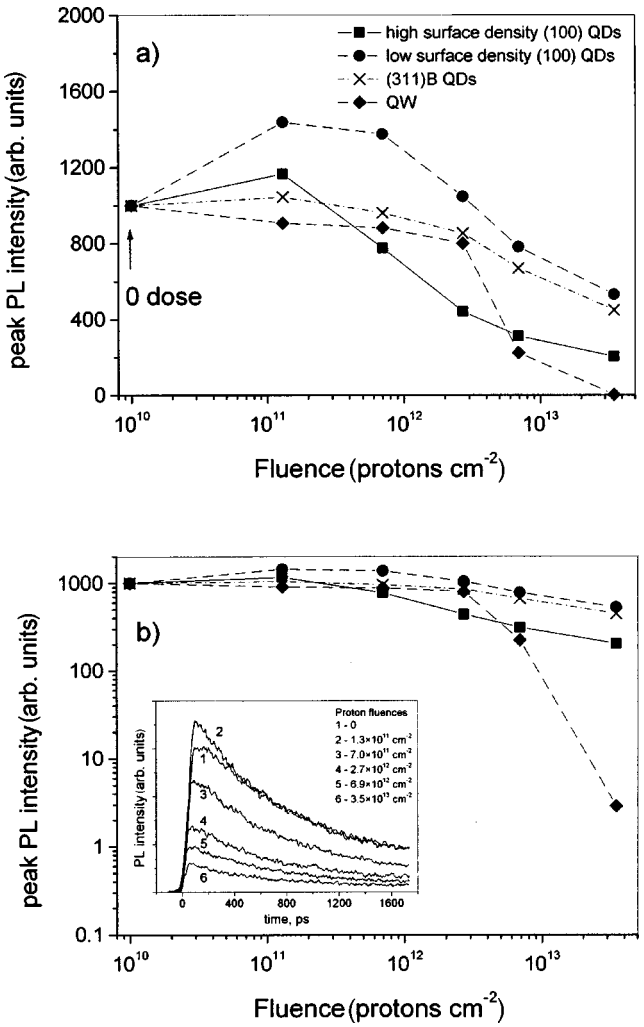

FIG. 1. PL peak intensities for different QD structures and for thin InGaAs QW as a function of proton fluence, shown in (a) linear, and (b) logarithmic scales. The inset shows transients of PL intensity vs time for high surface density InGaAs (100) QD's for different proton (1.5 MeV) fluences.

Figure 4 shows the expected ranges of hydrogen ions (protons) in GaAs calculated from "Trajectories and Ranges of Ions in Matter (TRIM)" [17] simulations. Also shown are the calculated numbers of total target displacement events per ion per angstrom at a depth of 100 nm in GaAs. An inverse relation between range and displacement defects created can be seen.

Additional continuous wavelength (CW) PL experiments were performed on InGaAs (100) QD's by varying the energy of optical excitation. In this experiment, the goal was to use two additional excitation wavelengths (energies); in this way photoexcitation of carriers in the WL and the QD's (but not in the barriers) was achieved at 920 nm (1.348 eV), and, as the wavelength was tuned to 970 nm (1.278 eV), carriers were excited only in the QD's. This experiment allows differentiation between carriers generated in the WL and showing changes in the transfer process into the QD's, and changes in PL decay times for carrier photoexcited directly into the QD's. When 920-nm excitation was used, a similar

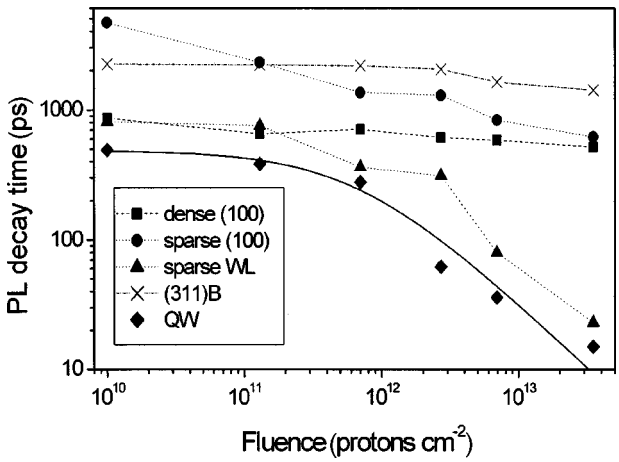

FIG. 2. PL decay times for the QD structures and InGaAs QW as a function of varying proton fluence. Solid line is a fit which takes into account carrier trapping to native and irradiation-induced defects.

PL intensity increase was observed as in the case of above band-gap excitation (similar to what is shown in Fig. 1), while for excitation in the dots the PL intensity for moderate irradiation fluences was irradiation independent.

IV. DISCUSSION

A. Carrier lifetimes and recombination

As can be seen, PL intensities and carrier lifetimes in QD's are much less affected by proton irradiation than in the QW (or the WL in the low-density QD structures), which implies that QD's are more radiation tolerant than QW's of the same composition. This increase in radiation hardness is significant, because QW based devices already represent a vast improvement in radiation hardness over bulk devices. For example, experiments performed with 50-MeV protons on different types of light emitting diodes (LED's) used in optocoupler applications, showed significantly worse degradation for the *pn*-junction based amphoterically doped (Si)

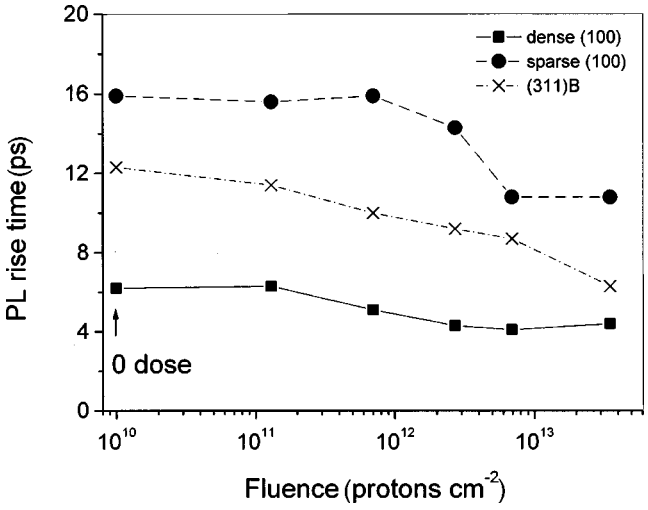

FIG. 3. PL rise times for all QD structures vs proton fluence.

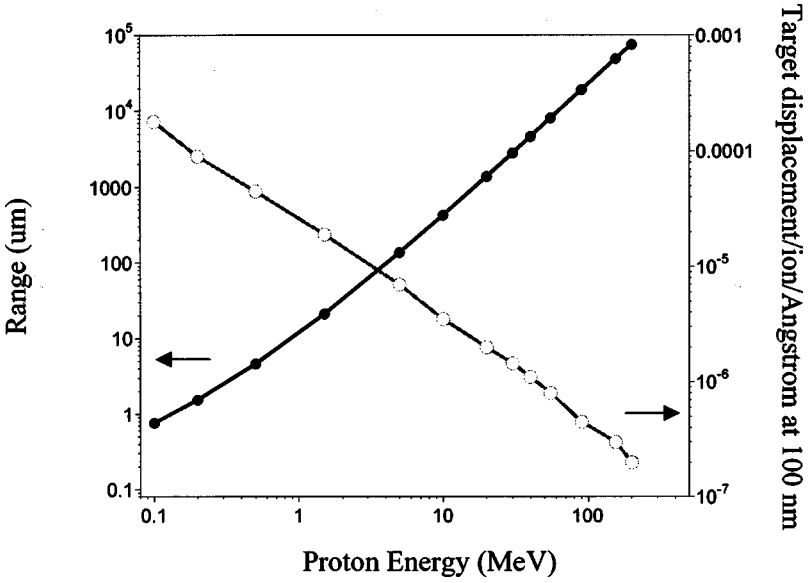

FIG. 4. Calculated ranges in GaAs for 1.5-MeV protons (solid symbol); and calculated displacement defects per ion per Å at a depth of 100 nm in GaAs (hollow symbols) as a function of proton beam energy.

GaAs LED's than for the GaAs/AlGaAs LED's based on QW's (also known as double-heterojunction LED's);[18,19] these studies demonstrated that LED's based on QW's showed over an order of magnitude greater tolerance to proton induced displacement damage when compared to the LED's based on *pn* junction geometries. An important difference for the QD and QW comparison here is that unlike the case reported for the LED study,[19] the initial emission from the QD's is stronger than from the QW, so initial brightness is not compromised in device applications.

A rough comparison between the present results and the cited earlier studies can be made using the calculated ratios of displacement events per ion per angstrom at the known active region depth. As is shown in Fig. 4, at a depth of 100 nm in GaAs, 1.5 MeV protons cause ~25 times more damage than 50-MeV protons. Since this damage ratio is an estimation, further experiments at higher proton energies should also be performed in some of these QD and QW structures for greater accuracy and in order to eliminate unforseen effects.

Similar trends in radiation tolerance are observed for all QD samples, and can be explained by the different level of confinement in the QW and QD structures. Unlike in QW's, carriers in QD's are not mobile, and their lifetime is reduced only by the defects created inside the dots. In the QW structures, the carriers can move in the QW plane, find a trap and be rapidly removed from the conduction/valence bands. On the other hand, carriers in the QD's are confined in all three dimensions and are not mobile. Once a carrier are trapped into a QD, only defects created inside or near the dot contribute to reduction of the carrier lifetime, as will be discussed in more detail below.

The measured dependence of the PL decay time on irradiation dose can be used to evaluate trapping rates to the native and radiation-induced defects. The full line in Fig. 2 corresponds to the relation $\tau = 1/(B_0 + B_i)$, where τ is the PL decay time and B_0 and B_i are carrier trapping coefficients to the native and irradiation-induced centers, respectively. In the as-grown QW sample, the PL decay time is 500 ps. This time is mostly determined by the nonradiative recombination (the radiative recombination time in InGaAs/GaAs QW's at 80 K is of the order of nanoseconds).[20] Considering that in the 1-nm-thin QW most of the electron wave function is spread into the barriers,[21] carrier lifetime in the thin QW is mainly determined by traps within the barriers. The main electron traps in MOCVD grown GaAs are ionized EL2 donors.[22] This trap concentration can be evaluated from the known EL2 electron capture cross section[22] and the PL decay time measured in the QW sample, which gives a native trap concentration of $\sim 2\times10^{15}$ cm^{-3}. This simple model describes the experimental results rather well, and it shows that at proton fluences of 1×10^{12} cm^{-2}, the trapping rates to the native and radiation-induced defects are equal.

It is well known that proton irradiation in GaAs produces a wide spectrum of displacement defects including As antisites (EL2), As vacancies, and As vacancy–interstitial complexes.[22,23] Ionized EL2 defects are considered to be the main electron traps in proton-irradiated samples.[24] Moreover, other electron traps, such as E4, present at concentrations comparable to that of EL2 in proton irradiated samples,[22,23] have similar electron capture cross sections as the EL2. The same or similar origin of traps and capture cross sections in the as-grown and irradiated QW samples allow us to make an estimation of irradiation-induced defect concentration. For the proton fluence of 1×10^{12} cm^{-2}, for which the capture coefficients to the native and induced defects are equal, the irradiation-related active trap concentration in the vicinity of the QW should be about 2×10^{15} cm^{-3}. A comparison between these values and the estimated radiation induced defect centers obtained from the fit of the experimental data on PL decay times is now possible, and it shows some interesting findings. Figure 4 shows that 2×10^{-5} displacement defects are created per each energetic ion (proton) per each angstrom depth in the vicinity of 100-nm depth in GaAs. For the proton fluence of 1×10^{12} cm^{-2}, this will create 2×10^{7} cm^{-2} defects per Å depth, or 2×10^{15} defects/cm^3 (at 100-nm depth). This number coincides with the concentra-

tion of irradiation-induced defects evaluated from the PL decay times, which confirms that displacement defects in proton-irradiated samples indeed act as efficient carrier traps.

For a QD of lens shape, 25 mm in diameter and 4 mm in height, the dot volume is equal to 1.1×10^{-18} cm^3. For the irradiation-induced defect concentration of 2×10^{15} defects/cm^3 and uniform defect distribution, the average volume containing a single defect is 5×10^{-16} cm^3. The ratio between this volume and the dot volume gives the fraction of dots containing a defect. For proton fluence of 1×10^{12} cm^{-2}, this fraction is only 0.002. Even for the highest irradiation fluence used in the current study, the fraction of dots containing a displacement defect is only 0.08. Of course, the carriers might be trapped from the dots not only by defects, created inside the dots, but also by defects situated close to the dots. For the deep traps, however, the wave functions are well localized, and an efficient carrier transfer from dots into defects may be expected for only a distance of a few nanometers or so.[25] This simple geometrical exercise clearly reveals the origin of radiation tolerance of the QD structures, however, one should be aware that it applies only to carriers confined in all three dimensions.

B. Carrier transfer into the QD's

The decrease in QD PL rise times seen in Fig. 3 is mainly attributed to the reduction of carrier transport time (due to carrier trapping to defects) in the barriers, from which the carriers are collected into the QD's. The shorter capture times and lower total PL intensities simply reflect the fact that QD's collect only carriers generated closer to the dots, since electron-hole pairs excited further away from the QD's can recombine nonradiatively at radiation-induced defect centers.

The surprising enhancement of the PL intensity from QD structures seen at low to intermediate proton fluences can been explained by two possible mechanisms:

(i) Reduction of the phonon bottleneck by defect assisted phonon emission has been proposed[26] as a mechanism to explain the bright PL emission in QD's. Perhaps in dots with defect free interfaces, introduction of deep level defects as those originated from displacement damage might provide additional relaxation path[27] to the ground level and therefore increase the luminescence emission.

(ii) Several recent experiments have identified capture barriers (also known as potential or energy barriers) at the QD/barrier and QD/WL interfaces.[28–30] These barriers are attributed to strain effects and have been shown to affect or inhibit carrier transfer into the quantum dots. If irradiation-created defects near the QD/barrier interface, where the potential barriers have been identified, increase the efficiency of carrier transfer into the QD's, PL emission from QD states would increase. Increased carrier collection from the WL to the QD's may occur due to an additional channel of carrier transfer, namely, trapping via radiation-induced defects. During such a process, carriers are first trapped from the WL into defect levels and then tunnel into the dots.

The results presented here allow an unambiguous determination of which is these two mechanisms prevails and can best explain the observed PL intensity increase seen after fluences $\sim10^{11}$ and 10^{12} protons/cm^2. Elucidation of the physical mechanism responsible for this unusual PL increase can be achieved by examination of the data presented in Figs. 1 and 3; as well as from the PL intensity measurements performed using laser excitation at wavelengths above the WL energy and below the WL energy (at 920 and 970 nm).

If the observed PL increase is due to the first mechanism proposed (i), then we should observe:

(a) A decrease in PL decay time at the same proton fluences that show a PL intensity increase with above bandgap excitation, and;

(b) A similar increase in PL intensity with low to intermediate proton fluences when using excitation energies below the WL energy.

Since neither (a) nor (b) are observed, our results suggest rather an increase in the efficiency with which the carriers are transferred into the QDs. This should occur due to irradiation defect-assisted transfer from the WL to the QD's. Here we should note that these defects should have shallower energy levels (with a confinement energy less or equal to that of a dot) compared to the deep carrier traps discussed above. A possible candidate is the level E2, formed by an As vacancy and an interstitial.[24]

One could question why is the defect-assisted carrier transfer into the dots efficient for irradiation doses (and defect concentrations) for which the opposite effect, the carrier trapping from the dots is not. First of all, the shallow and deep defect concentrations might be different, as well as the character of their dependence on irradiation dose. A complicated dependence of trap concentration on irradiation dose, different for shallow and deep traps, has been observed for proton-irradiated bulk GaAs.[22] Besides, the wave-function localization volume for the shallow traps may differ from that of the deep by orders of magnitude increasing the length of efficient defect-dot interaction.[25] Finally, the rate of carrier transfer between defect and quantum dot levels strongly depends on their energy difference.[31] The fact that we observe enhancement of the PL intensity in some, but not all the samples, like those grown on (311) B GaAs, suggests a resonant character of the effect. A more detailed knowledge of the energies, concentrations, and capture cross sections of the radiation-induced defects introduced in the vicinity of the QD's should aid further understanding of the discussed processes.

V. CONCLUSIONS

In summary, comparison of PL intensities and decay times between QW and various types of InGaAs/GaAs quantum dots after 1.5-MeV proton irradiation shows significantly greater radiation hardness in quantum dots. We have observed that carrier lifetimes in QD's are not strongly affected

by displacement damage defects introduced by proton irradiation. This is explained by better carrier localization in the QD's than in QW's. Enhancement of the PL intensity at low to moderate radiation doses suggests a more effective carrier transfer from the WL into the QD's after irradiation. This may occur due to an additional channel of carrier trapping from the barriers and the WL into the QD's, namely, trapping from the WL to the QD's via radiation-induced defects.

ACKNOWLEDGMENTS

Part of this research was carried out at the Jet Propulsion Laboratory, California Institute of Technology, under a contract with the National Aeronautics and Space Administration. Financial support from the Swedish Foundation for International Cooperation in Research and Higher Education (STINT) is gratefully acknowledged.

[1] S. Muto, Jpn. J. Appl. Phys., Part 2 **34**, L210 (1995).
[2] M. Shima, Y. Sakuma, T. Futatsugi, Y. Awano, and N. Yokoyama, IEEE Trans. Electron Devices **47**, 2054 (2000).
[3] A. O. Orlov, I. Amlani, G. Toth, C. S. Lent, G. H. Bernstein, and G. L. Snyder, Appl. Phys. Lett. **74**, 2875 (1999).
[4] Y. Arakawa and H. Sakaki, Appl. Phys. Lett. **40**, 939 (1982).
[5] G. Park, O. B. Shchekin, D. L. Huffaker, and D. G. Deppe, IEEE Photonics Technol. Lett. **12**, 230 (2000).
[6] X. Huang, A. Stintz, C. P. Hains, G. T. Liu, J. Cheng, and K. J. Malloy, Electron. Lett. **36**, 41 (2000).
[7] H. Saito, K. Nishi, A. Kamei, and S. Sugou, IEEE Photonics Technol. Lett. **12**, 1298 (2000).
[8] H. C. Liu, M. Gao, J. McCaffrey, Z. R. Wasilewski, and S. Fafard, Appl. Phys. Lett. **78**, 79 (2001).
[9] R. Leon, G. M. Swift, B. Magness, W. A. Taylor, Y. S. Tang, K. L. Wang, P. Dowd, and Y. H. Zhang, Appl. Phys. Lett. **76**, 2074 (2000).
[10] W. V. Schoenfeld, C. H. Chen, P. M. Petroff, and E. L. Hu, Appl. Phys. Lett. **73**, 2935 (1998).
[11] N. A. Sobolev, A. Cavaco, M. C. Carmo, M. Grundmann, F. Heinrichsdorff, and D. Bimberg, Phys. Status Solidi B **224**, 93 (2001).
[12] P. G. Piva, R. D. Goldberg, I. V. Mitchell, D. Labrie, R. Leon, S. Charbonneau, Z. R. Wasilewski, and S. Fafard, Appl. Phys. Lett. **77**, 624 (2000).
[13] C. Ribbat, R. Sellin, M. Grundmann, D. Bimberg, N. A. Sobolev, and M. C. Carmo, Electron. Lett. **37**, 174 (2001).
[14] R. Leon, C. Lobo, J. Zou, T. Romeo, and D. J. H. Cockayne, Phys. Rev. Lett. **81**, 2486 (1998).
[15] C. Lobo, N. Perret, D. Morris, J. Zou, D. J. H. Cockayne, M. B. Johnston, M. Gal, and R. Leon, Phys. Rev. B **62**, 2737 (2000).
[16] R. Leon, S. Marcinkevičius, X. Z. Liao, J. Zou, D. J. H. Cockayne, and S. Fafard, Phys. Rev. B **60**, R8517 (1999).
[17] http://physics.nadn.navy.mil/physics/Faculty/Ziegler/home.htm
[18] B. G. Rax, C. I. Lee, A. H. Johnston, and C. E. Barnes, IEEE Trans. Nucl. Sci. **43**, 3167 (1996).
[19] A. H. Johnston, B. G. Rax, L. E. Selva, and C. E. Barnes, IEEE Trans. Nucl. Sci. **46**, 1781 (1999).
[20] H. Yu, C. Roberts, and R. Murray, Mater. Sci. Eng., B **35**, 129 (1995).
[21] P. Borri, W. Langbein, and J. M. Hwam, Phys. Rev. B **59**, 2215 (1999).
[22] H. H. Tan, J. S. Williams, and C. Jagadish, J. Appl. Phys. **78**, 1481 (1995).
[23] F. H. Eisen, K. Bachem, E. Klausman, K. Koehler, and R. Haddad, J. Appl. Phys. **72**, 5593 (1992).
[24] R. Ferrini, M. Galli, G. Guizzetti, M. Patrini, F. Nava, C. Canali, and P. Vanni, Appl. Phys. Lett. **71**, 3084 (1997).
[25] A. Blom, M. A. Odnoblyudov, I. N. Yassievich, and K. A. Chao, Phys. Rev. B **65**, 155302 (2002).
[26] P. C. Sercel, Phys. Rev. B **51**, 14 532 (1995); D. F. Schroeter, D. J. Griffits, and P. C. Sercel, *ibid.* **54**, 1486 (1996).
[27] H. Benisty, C. M. Sotomayor-Torres, and C. Weisbuch, Phys. Rev. B **44**, 10 945 (1991).
[28] C. Lobo, R. Leon, S. Marcinkevičius, W. Yang, P. C. Sercel, X. Z. Liao, J. Zou, and D. J. H. Cockayne, Phys. Rev. B **60**, 16 647 (1999).
[29] S. Marcinkevičius and R. Leon, Appl. Phys. Lett. **76**, 2406 (2000).
[30] H. L. Wang, F. H. Yang, S. L. Feng, H. J. Zhu, D. Ning, H. Wang, and X. D. Wang, Phys. Rev. B **61**, 5530 (2000).
[31] X.-Q. Li and Y. Arakawa, Phys. Rev. B **56**, 10 423 (1997).